

WEAKLY NONLINEAR STABILITY ANALYSIS OF A THIN MAGNETIC FLUID DURING SPIN COATING

Sen Yung Lee ^{a,*}, Ming Che Lin ^b

*Corresponding author, [†] Presenting author

^a Department of Mechanical Engineering, National Cheng Kung University, Tainan 70101, Taiwan
E-mail: sylee@mail.ncku.edu.tw

^b Department of Mechanical Engineering, National Kaohsiung University of Applied Sciences,
Kaohsiung 807, Taiwan
E-mail: limit168@cc.kuas.edu.tw

ABSTRACT

This paper investigates the stability of a thin electrically conductive fluid under the applied uniform magnetic field during spin coating. A generalized nonlinear kinematic model is derived by the long-wave perturbation method to represent the physical system. After linearizing the nonlinear evolution equation, the method of normal mode is applied to the linear stability. The weakly nonlinear dynamics of a film flow are studied by the multiple scales method. The Ginzburg-Landau equation is determined to discuss the necessary conditions of the various states of the critical flow states, namely sub-critical stability, sub-critical instability, supercritical stability and supercritical explosion. The study reveals that the rotation number and the radius of the rotating circular disk generate similar destabilizing effects but Hartman number gives a stabilizing effect. Moreover, the optimum conditions can be found to alter stability of the film flow by controlling the applied magnetic field.

1. INTRODUCTION

The study of magnetohydrodynamic (MHD) effects is important for a wide range of situations, varying from MEMS technology, plasma engineering, and thin film materials technology [1-3]. In fact, to stabilize the film flow by applying a magnetic field has more advantages as follows: (1) neither electrical nor mechanical contacts with the fluid are necessary, (2) an active control of a technological process is simple.

Several researchers performed hydromagnetic stability analyses of film flows on a rotating disk [4-8]. In the present study, the authors present a weakly nonlinear stability analysis of a thin electrically conductive fluid under the applied uniform magnetic field on a rotating disk, namely spin coating. The induced magnetic field is neglected by assuming that the magnetic Reynolds number $\ll 1$ [7] during spin coating. It is also assumed that the disk radius is much larger than the film thickness. Therefore, the peripheral effect is neglected by comparing with total film area. It is focused that the effects of

stability due to centrifugal forces and MHD effects were revealed in the region near the rotating axis. The influence of the rotational motion, the disk size and the Hartmann number on the equilibrium finite amplitude is studied and characterized mathematically. In an attempt to verify the computational results and to illustrate the effectiveness of the proposed modelling approach, several numerical examples are presented.

2. MATHEMATICAL FORMULATION

Consider the axisymmetric flow of a thin electrically conductive fluid flowing on a rotating circular disk which rotates with constant angular velocity Ω^* under an applied magnetic field B_0^* . The external uniform magnetic field is applied perpendicular to the plane of the disk (see Fig. 1). A variable with a superscript $*$ represents a dimensional quantity. Here the cylindrical polar coordinate axes r^*, θ^*, z^* are chosen as the radial direction, the circumferential direction and the axial direction, respectively. All associated physical properties and the rate of film flow are assumed to be constant (i.e. time-invariant). Let u^* and w^* be the velocity components in the radial direction r^* and the perpendicular direction z^* of the disk, respectively. According to the experimental observation by Takamasa and Kobayashi [9], it is reasonable to be assumed to ignore the circumferential effect when the liquid film is very thin ($h^* \ll r^*$). For simplification, we take the fluid velocity in the thinning film to be independent of θ^* . For small magnetic Reynolds number, the electromagnetic force F_m is $\sigma B_0^{*2} u^*$ [7, 8], when imposed and induced electric fields are negligible and the only applied magnetic field B_0^* . The MHD governing equations of motion can be expressed as

$$\frac{1}{r^*} \frac{\partial(r^* u^*)}{\partial r^*} + \frac{\partial w^*}{\partial z^*} = 0 \quad (1)$$

$$\rho \left(\frac{\partial u^*}{\partial t^*} + u^* \frac{\partial u^*}{\partial r^*} + w^* \frac{\partial u^*}{\partial z^*} - \frac{v^{*2}}{r^*} \right) = - \frac{\partial p^*}{\partial r^*} + \frac{\mu}{\rho} \left(\frac{\partial^2 u^*}{\partial r^{*2}} + \frac{1}{r^*} \frac{\partial u^*}{\partial r^*} + \frac{\partial^2 u^*}{\partial z^{*2}} - \frac{u^*}{r^{*2}} \right) - \sigma B_0^{*2} u^* \quad (2)$$

$$\frac{\partial w^*}{\partial t^*} + u^* \frac{\partial w^*}{\partial r^*} + w^* \frac{\partial w^*}{\partial z^*} = - \frac{1}{\rho} \frac{\partial p^*}{\partial z^*} - g + \frac{\mu}{\rho} \left(\frac{1}{r^*} \frac{\partial}{\partial r^*} \left(r^* \frac{\partial w^*}{\partial r^*} \right) + \frac{\partial^2 w^*}{\partial z^{*2}} \right) \quad (3)$$

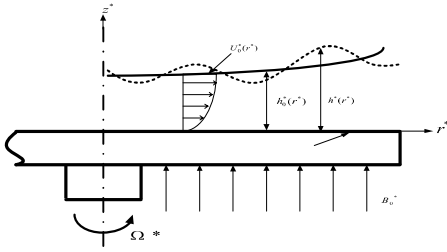


Figure 1 Schematic diagram of a thin MHD fluid flowing on a rotating circular disk

where v^* is tangential velocity, ρ is constant fluid density, p^* is fluid pressure, g is acceleration due to gravity, μ is fluid dynamic viscosity and B_0^* is magnetic flux density.

On the disk surface $z^* = 0$, the boundary conditions are treated as no-slip as

$$u^* = 0 \quad (4)$$

$$w^* = 0 \quad (5)$$

On the free surface $z^* = h^*$, the boundary condition approximated by the vanishing of shear stress is expressed as

$$\left(\frac{\partial u^*}{\partial z^*} + \frac{\partial w^*}{\partial r^*}\right)\left(1 - \left(\frac{\partial h^*}{\partial r^*}\right)^2\right) - 2^* \left(\frac{\partial u^*}{\partial r^*} - \frac{\partial w^*}{\partial z^*}\right)\left(\frac{\partial h^*}{\partial r^*}\right) = 0 \quad (6)$$

The normal stress condition obtained by solving the balance equation in the direction normal to the free surface is given as

$$p^* + 2\mu\left(1 + \left(\frac{\partial h^*}{\partial r^*}\right)^2\right)^{-1} \left[\frac{\partial h^*}{\partial r^*} \left(\frac{\partial u^*}{\partial z^*} + \frac{\partial w^*}{\partial r^*}\right) - \frac{\partial w^*}{\partial z^*} - \frac{\partial u^*}{\partial r^*} \left(\frac{\partial h^*}{\partial r^*}\right)^2 \right] + S^* \frac{\partial^2 h^*}{\partial r^{*2}} \left[1 + \left(\frac{\partial h^*}{\partial r^*}\right)^2 \right]^{-3/2} = p_a^* \quad (7)$$

The kinematic condition that ensures the flow does not travel across a free surface can be given as

$$\frac{\partial h^*}{\partial t^*} + \frac{\partial h^*}{\partial r^*} u^* - w^* = 0 \quad (8)$$

where h^* is the local film thickness, S^* is surface tension and p_a^* is atmosphere pressure. By introducing a stream function φ^* , the dimensional velocity components can be expressed as

$$u^* = \frac{1}{r^*} \frac{\partial \varphi^*}{\partial z^*}, \quad w^* = -\frac{1}{r^*} \frac{\partial \varphi^*}{\partial r^*} \quad (9)$$

The following variables are used to form the dimensionless governing equations and boundary conditions

$$z = \frac{z^*}{h_0^*}, \quad r = \frac{ar^*}{h_0^*}, \quad t = \frac{at^* u_0^*}{h_0^*}, \quad h = \frac{h^*}{h_0^*}, \quad \varphi = \frac{\alpha \varphi^*}{u_0^* h_0^{*2}}, \quad p = \frac{p^* - p_a^*}{\rho u_0^{*2}} \quad (10)$$

$$Re = \frac{u_0^* h_0^*}{\nu}, \quad Fr = \frac{gh_0^*}{u_0^{*2}}, \quad S = \frac{S^*}{\rho u_0^{*2} h_0^*}, \quad m = \frac{\sigma B_0^{*2} h_0^{*2}}{\mu}, \quad \alpha = \frac{2\pi h_0^*}{\lambda} \quad (10)$$

where h_0^* is the average film thickness, α is the dimensionless wave number, u_0^* is the scale of velocity, ν is the kinematic viscosity, Re is the Reynolds number, Fr is the Froude number, m is the Hartmann number and λ is the wavelength. In order to investigate the effect of angular

velocity, Ω^* on the stability of the flow field, it is assumed that the tangential velocity is constant [7, 8] throughout the radial direction in the thin film, i.e. $v^* = r^* \Omega^*$. The dimensionless parameter Ro (rotation number) is defined as

$$Ro = \frac{\Omega^* h_0^*}{u_0^*} \quad (11)$$

In terms of these non-dimensional variables, the equations of motion can be expressed as

$$r^{-1} \varphi_{zz} = -Re r Ro^2 + r^{-1} m \varphi_z + \alpha Re (p_r + r^{-1} \varphi_z + r^{-2} \varphi_z \varphi_z - r^{-3} \varphi_z^2 - r^{-2} \varphi_z \varphi_z) + O(\alpha^2) \quad (12)$$

$$p_z = -Fr + \alpha (-Re^{-1} r^{-1} \varphi_{zz}) + O(\alpha^2) \quad (13)$$

Using the non-dimensional variables, the boundary conditions at the surface of disk $z=0$ reduce to

$$\varphi = \varphi_r = \varphi_z = 0 \quad (14)$$

And the boundary conditions at the free surface of disk $z=h$ become

$$r^{-1} \varphi_{zz} = \alpha^2 [r^{-1} \varphi_{rr} - r^{-2} \varphi_r + 2h_r (1 - \alpha^2 h_r^2)^{-1} (2r^{-1} \varphi_{rz} - r^{-2} \varphi_z)] \quad (15)$$

$$p = -S \alpha^2 h_{rr} (1 + \alpha^2 h_r^2)^{-3/2} + \alpha [-2Re^{-1} (1 + \alpha^2 h_r^2)^{-1} (r^{-1} \varphi_z + r^{-1} \varphi_z h_r)] + O(\alpha^2) \quad (16)$$

$$h_r + r^{-1} h_r \varphi_z + r^{-1} \varphi_r = 0 \quad (17)$$

Hence the term $\alpha^2 S$ can be treated as a quantity of zeroth order [10, 11]. The long-wave length modes (i.e. a small wave number, α) is considered in the present analysis, this can be done by expanding the stream function and flow pressure in terms of some small wave number ($\alpha \ll 1$) as

$$\varphi = \varphi_0 + \alpha \varphi_1 + O(\alpha^2) \quad (18)$$

$$p = p_0 + \alpha p_1 + O(\alpha^2) \quad (19)$$

The flow conditions of the thin film can be obtained by inserting the above expressions into Eqs. (12)–(16) and then solving systematically the resulting equations. By collecting all terms of zeroth order α^0 and first order α^1 in the above governing equations and boundary conditions, the zeroth and first order solutions are inserted into the dimensionless free surface kinematic equation to yield the following generalized nonlinear kinematic equation

$$h_t + A(h)h_r + B(h)h_{rr} + C(h)h_{rrr} + D(h)h_{rrrr} + E(h)h_r^2 + F(h)h_r h_{rr} = 0 \quad (20)$$

where $A(h)$, $B(h)$, $C(h)$, $D(h)$, $E(h)$ and $F(h)$ are given in Appendix A.

3. STABILITY ANALYSIS

The dimensionless film thickness when expressed in perturbed state can be given as

$$h(r, t) = 1 + \eta(r, t) \quad (21)$$

Where η is a perturbed quantity to the stationary film thickness. Substituting the value of $h(r, t)$ into the evolution Eq. (20) and all terms up to the order of η^3 are collected, the evolution equation of η becomes

$$\eta_t + A\eta_r + B\eta_{rr} + C\eta_{rrr} + D\eta_{rrrr} + E\eta_r^2 + F\eta_r \eta_{rr} = (A'\eta + \frac{A}{2}\eta^2)\eta_r + (B'\eta + \frac{B}{2}\eta^2)\eta_{rr} + (C'\eta + \frac{C}{2}\eta^2)\eta_{rrr} + (D'\eta + \frac{D}{2}\eta^2)\eta_{rrrr} + (E + E'\eta)\eta_r^2 + (F + F'\eta)\eta_r \eta_{rr} + O(\eta^4) \quad (22)$$

where the values of A , B , C , D , E , F and their derivatives are all evaluated and as following at the dimensionless height of the film $h=1$.

3.1 LINEAR STABILITY ANALYSIS

When the nonlinear terms of Eq. (22) are neglected, the linearized equation is given as

$$\eta_t + A\eta_r + B\eta_{rr} + C\eta_{rrr} + D\eta_{rrrr} = 0 \quad (23)$$

In order to use the normal mode analysis, we assume that $\eta = a \exp[i(r - dt)] + c.c.$ (24)

where a is the perturbation amplitude, and c.c. is the complex conjugate counterpart. The complex wave celerity, d is given as $d = d_r + id_i = (A - C) + i(B - D)$ (25)

where d_r and d_i are regarded as the linear wave speed and linear growth rate of the disturbance respectively. The solution of the disturbance about $h(r, t) = 1$ is asymptotically stable or unstable according as $d_i < 0$ or $d_i > 0$. This is equivalent to the inequality $B < D$ or $B > D$.

3.2 WEAKLY NONLINEAR STABILITY ANALYSIS

Nonlinear effects, when they are weak enough, do not fundamentally alter the nature of the motion. A weakly nonlinear solution can be usefully expressed as weak stability or instability, but the definition is restricted to some neighborhood of critical value. In this paper the authors are interested in investigating the existence of the supercritical and subcritical regions. In order to characterize the weakly nonlinear behaviors of thin film flows, the method of multiple scales [12] is employed here and the resulting Ginzburg-Landau equation [13] can be derived following the same procedure as Chen [11] and Cheng and Lin [14].

$$\frac{\partial a}{\partial t_2} + D_1 \frac{\partial^2 a}{\partial r_1^2} - \varepsilon^{-2} d_i a + (E_1 + iF_1) a^2 \bar{a} = 0 \quad (26)$$

where ε is a small perturbation parameter, $t_2 = \varepsilon^2 t$, $r_1 = \varepsilon r$, and

$$e = e_r + ie_i = \frac{(B' - D' + E - F)(16D - 4B) + 6C(A' - C')}{(16D - 4B)^2 + 36C^2} + i \frac{6C(B' - D' + E - F) - (A' - C')(16D - 4B)}{(16D - 4B)^2 + 36C^2} \quad (27)$$

$$D_1 = [(B - 6D) + i(3C)] \quad (28)$$

$$E_i = (-5B' + 17D' + 4E - 10F)e_r - (A' - 7C')e_i + (-\frac{3}{2}B' + \frac{3}{2}D' + E' - F') \quad (29)$$

$$F_i = (-5B' + 17D' + 4E - 10F)e_r + (A' - 7C')e_i + \frac{1}{2}(A' - C') \quad (30)$$

The overhead bar appearing in Eq. (26) stands for the complex conjugate of the same variable. Equation (26) can be used to investigate the weak nonlinear behaviour of a fluid film flow. In order to solve for Eq. (26), we assume a filtered wave with no spatial modulation, so the filtered wave can be expressed as

$$a = a_0 \exp[-ib(t_2)t_2] \quad (31)$$

After substituting Eq. (31) into Eq. (26), one can obtain

$$\frac{\partial a_0}{\partial t_2} = (\varepsilon^{-2} d_i - E_1 a_0^2) a_0 \quad (32)$$

$$\frac{\partial [b(t_2)t_2]}{\partial t_2} = F_1 a_0^2 \quad (33)$$

The associated wave amplitude εa_0 in the supercritical stable region is derived and given as

$$\varepsilon a_0 = \sqrt{\frac{d_i}{E_1}} \quad (34)$$

If $E_1 = 0$, then Eq. (32) is reduced to a linear equation. The second term on the right-hand side of Eq. (32) is due to nonlinearity and may moderate or accelerate the exponential growth of the linear disturbance according to the signs of d_i and E_1 . Equation (33) is used to modify the perturbed wave speed caused by infinitesimal disturbances appearing in the nonlinear system. The Ginzburg-Landau equation can be used to characterize various flow states, with the results summarized and presented as a Landau table [15].

4. NUMERICAL EXAMPLES

In order to study the effects of dimensionless radius, rotation number and Hartman number on the stability of a thin flow, we select randomly but within specified ranges physical parameters for numerical experiment. The ranges for these parameters are based on published reasonable ranges for these parameters [10, 11, 14]. More specifically, these parameters and their values include: (1) Reynolds number (range from 0 to 15); (2) Dimensionless perturbation wave numbers (range from 0 to 0.12); (3) Rotation number (any one of the three values 0.15, 0.175 and 0.2); (4) Dimensionless radius (any one of the three values 10, 15 and 20). (5) Hartman number (any one of the three values 0, 0.05, 0.1 and 0.15). Other of our parameters are treated as constants for all numerical computations since we are considering practical spin coating systems in which these variables are not expected to undergo significant variation. In practice, the parameter S is a large value. Further, for simplification analysis, $\alpha^2 S \cdot Re$ and Fr are taken to be of the same order ($O(1)$) [11, 14], so the values of some dimensionless parameters are taken as, a constant dimensionless surface tension $S = 6173.5$ and $Fr = 9.8$.

4.1 LINEAR STABILITY ANALYSIS

By setting $d_i = 0$ in the linear stability analysis, the neutral stability curve can be determined easily from Eq. (25). The $\alpha^2 S$ - Re plane is divided into two different characteristic regions by the neutral stability curve. One is the linearly stable region where small disturbances decay with time and the other is the linearly unstable region where small perturbations grow as time increases. Figure 2(a) shows that the stable region decreases and unstable region increases with an increase of rotation number. Figure 2(b) shows that the stable region decreases and unstable region increases with increasing radius of the circular disk. The reason for this phenomenon is the existence of the centrifugal force term, which is a radius-related force in the governing equation. Increasing the radius and the rotation number results in accelerated growth of the linear disturbance due to the centrifugal force. Figure 2(c) shows that the stable region increases and unstable region decreases with an increase of Hartman number. The reason for this phenomenon is the Lorentz forces can modify the velocity field and moderate the growth of the linear disturbance. Hence one

2 Topics

can say that in linear stability analysis rotation number and the radius of circular disk generate similar destabilizing effects but Hartman number gives a stabilizing effect.

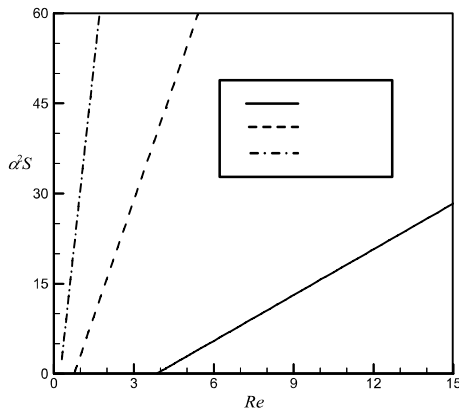


Figure 2(a) Linear neutral stability curves for three different Ro values at $r=10$ and $m=0.1$

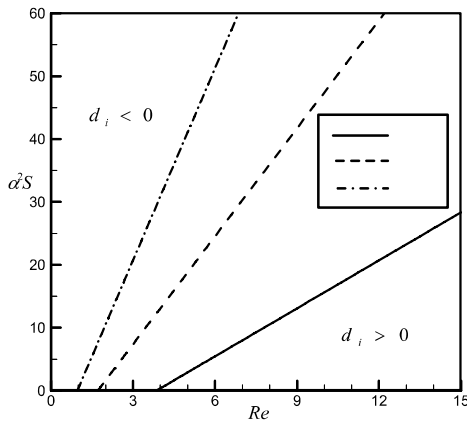


Figure 2(b) Linear neutral stability curves for three different r values at $m=0.1$ and $Ro=0.15$

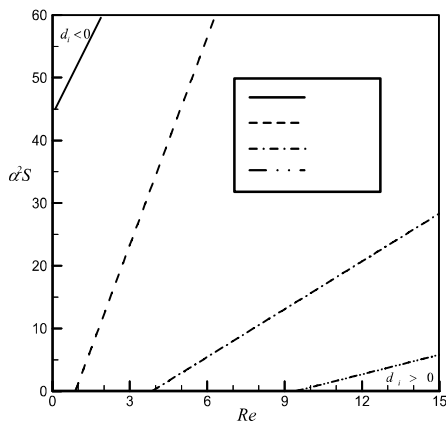


Figure 2(c) Linear neutral stability curves for three different m values at $r=10$ and $Ro=0.15$

4.2 WEAKLY NONLINEAR STABILITY ANALYSIS

Figures 3(a) to (c) reveal that various conditions for sub-critical instability ($d_i < 0, E_1 < 0$), sub-critical stability ($d_i < 0, E_1 > 0$), supercritical stability ($d_i > 0, E_1 > 0$) and supercritical explosion ($d_i > 0, E_1 < 0$).

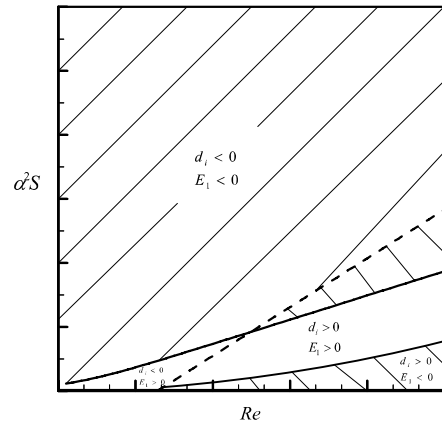


Figure 3(a) Neutral stability curves of MHD film flows for $r=10$, $Ro=0.15$ and $m=0.1$

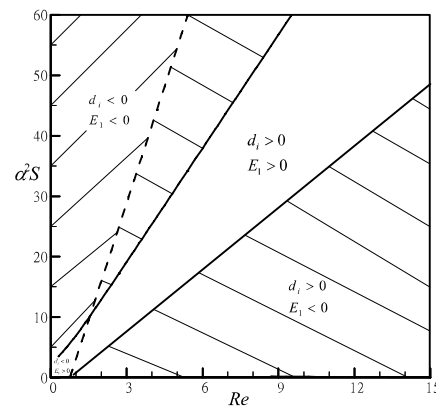


Figure 3(b) Neutral stability curves of MHD film flows for $r=10$, $Ro=0.175$ and $m=0.1$

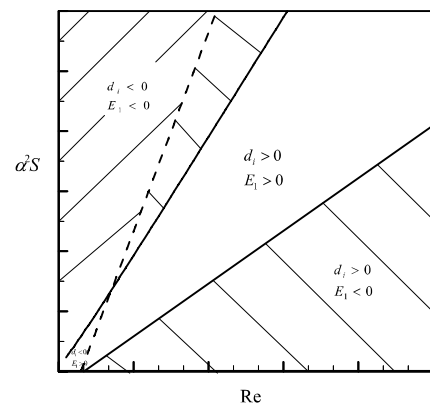


Figure 3(c) Neutral stability curves of MHD film flows for $r=10$, $Ro=0.15$ and $m=0.05$

Figure 4(a) shows the threshold amplitude in sub-critical instability region for various wave numbers with different Ro values at $Re=3$, $r=10$ and $m=0.1$. The results indicate that the threshold amplitude εa_0 becomes smaller as the value of rotation number (Ro) increases. Figure 4(b) shows the threshold amplitude in sub-critical instability region for various wave numbers with different Hartman number (m) values at $Re=3$, $r=10$ and $Ro=0.15$. The results indicate that the threshold amplitude εa_0 becomes smaller as the value of m decreases. The film flow which holds the higher threshold amplitude value will become more stable than those that hold smaller one. If the initial finite-amplitude disturbance is less than the threshold amplitude, the system will become conditionally stable.

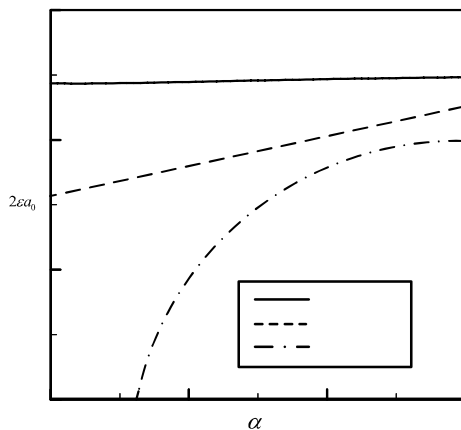


Figure 4(a) Threshold amplitude in sub-critical instability region for three different Ro values at $Re=3$, $r=10$ and $m=0.1$

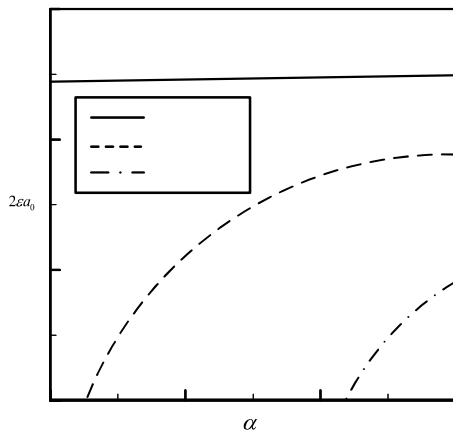


Figure 4(b) Threshold amplitude in sub-critical instability region for three different m values at $Re=3$, $r=10$ and $Ro=0.15$

Figure 5(a) shows the threshold amplitude in the supercritical stability region for various wave numbers with different Ro values at $Re=6$, $r=10$ and $m=0.1$. It is found that decreasing the rotation number will lower the threshold amplitude, whereupon the flow becomes relatively more stable.

Figure 5(b) shows the threshold amplitude in the supercritical stability region for various wave numbers with different m values at $Re=6$, $r=10$ and $Ro=0.15$. It is found that increasing of the Hartman number will lower the threshold amplitude, and the flow will become relatively more stable.

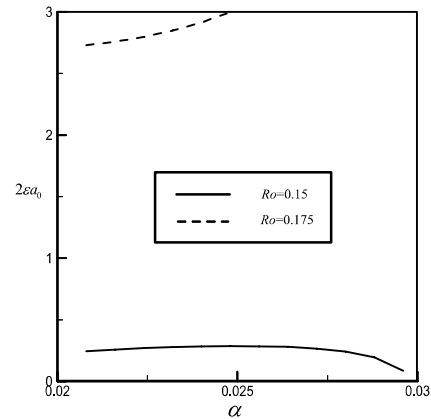


Figure 5(a) Threshold amplitude in supercritical stability region for two different Ro values at $Re=6$, $r=10$ and $m=0.1$

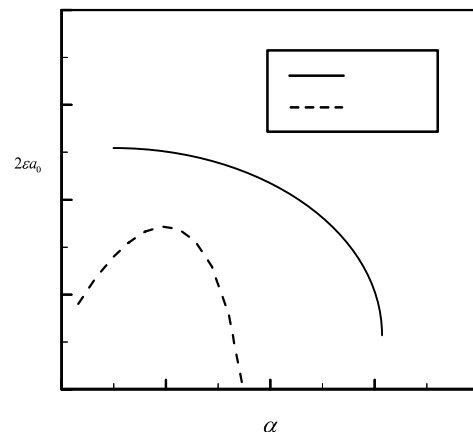


Figure 5(b) Threshold amplitude in supercritical stability region for two different m values at $Re=6$, $r=10$ and $Ro=0.15$

5. CONCLUDING REMARKS

The stability of a thin electrically conductive fluid under the applied uniform magnetic field during spin coating is investigated using the method of long-wave perturbation. On the basis of the results of numerical modeling, several conclusions can be drawn:

- (1). The modeling results indicate that the region of linearly stability becomes smaller for increasing rotation number or increasing radius. Hence one can say that in linear stability analysis rotation number and the radius of circular disk

2 Topics

generate similar destabilizing effects.

- (2).The modeling results also shows that the stable region increases and unstable region decreases with an increase of Hartman number. In linear stability analysis Hartman number gives a stabilizing effect.
- (3).Weakly nonlinear stability analysis has successfully revealed the sub-critical stability, sub-critical instability, supercritical stability and supercritical explosion regions for the flow patterns of a thin film on a rotating disk under the applied uniform magnetic field. It is found that in sub-critical instability region, the threshold amplitude εa_0 becomes smaller as the value of the rotation number becomes larger. When the initial finite-amplitude disturbance is less than the threshold amplitude, the flow will be conditionally stable.
- (4).It is also shows that in sub-critical instability region, the threshold amplitude εa_0 becomes larger as the value of the Hartman number becomes larger. The optimum conditions can be obtained that the system is used to increase stability of the film flow by controlling the applied magnetic field.

REFERENCES

- [1] Jang, J., and Lee, S.S., Theoretical and experimental study of MHD micropump, *Sensors and Actuators*, Vol.80, 2000, pp.84-89.
- [2] Herdrich, G., Auweter-Kurtz, M., Fertig, M., Nawaz, A. and Petkow, D., MHD flow control for plasma technology applications, *Vacuum*, Vol.80, 2006, pp.1167-1173.
- [3] Wasa, K., Kitabatake, M. and Adachi, H., Thin film materials technology: sputtering of compound materials, William Andrew Publishing., NY. 2004.
- [4] Benton, E.R., Loper, D.E., On the spin-up of an electrically conducting fluid, *J. Fluid Mech.* Part 1 39, 1969, pp.561-586.
- [5] Singh, K.D., An oscillatory hydromagnetic couette flow in a rotating system, *Math. Mech.*, Vol. 80 , 2000, pp.429-432.
- [6] Asghar S., Khan, S.B., Siddiqui, A.M. and Hayat, T., Exact solutions for magnetodynamic flow in a rotating fluid, *Acta Mech. Sinica*, Vol.28, 2002, pp.244-251.
- [7] Attia, H.A., Unsteady MHD flow near a rotating porous disk with uniform suction or injection, *Fluid Dynamics Research*, Vol.23, 1998, pp.283-290.
- [8] Hayat, T., Javed, T. and Sajid, M., Analytic solution for MHD rotating flow of a second grade fluid over a shrinking surface, *Phys. Letters A*, Vol.372, 2008, pp.3264-3273.
- [9] Takama, T., and Kobayashi K., Mearsuring interfacial waves on film flowing down tube inner wall using laser focus displacement meter, *Int. J. Multiphase Flow*, Vol.26, 2000, pp.1493-1507.
- [10] Tsai, J.S., Hung, C.Y. and Chen, C.K., Nonlinear hydromagnetic stability analysis of condensation film flow down a vertical plate, *Acta Mech.*, Vol.118, 1996, pp.197-212.
- [11] Chen, C.I., Non-linear stability characterization of the thin micropolar liquid film flowing down the inner surface of a rotating vertical cylinder, *Communications in nonlinear science and numerical simulation*, Vol. 12, 2007, pp.760-775.
- [12] Krishna, M.V.G. and Lin, S.P., Nonlinear stability of a viscous film with respect to three-dimensional side-band disturbance, *The Physics of Fluids*, Vol.20, 1977, pp.1039-1044.
- [13]Ginzburg, V.L. and Landau, L.D., Theory of Superconductivity, *J. of Experiential Theoretic Physics* (USSR), Vol.20, 1950, pp.1064-1082.
- [14] Cheng, P. J. and Lin, T.W., Surface waves on viscoelastic magnetic fluid film flow down a vertical column, *Int. J. Engineering Science*, Vol.45, 2007, pp.905-922.
- [15] Eckhaus, W., Studies in Nonlinear Stability, Springer, Berlin, 1965.

APPENDIX A

$$\begin{aligned}
 A(h) &= \frac{1}{12m^{7/2}r} (Sech(h\sqrt{m}))^2 (2\sqrt{m}(-3m^2r^2Ro^2 - Fr \cdot h^3m^3\alpha \\
 &+ 30r^2 Re^2 Ro^4\alpha + (h-18)h^2m \cdot r^2 Re^2 Ro^4\alpha + \\
 &(3m^2r^2Ro^2 - Fr \cdot h^3m^3\alpha + h^2(5h-6)m \cdot r^2 Re^2 Ro^4\alpha)Cosh(2h\sqrt{m})) \\
 &- r^2 Re^2 Ro^4\alpha(2h \cdot m(42 + h(9-14h \cdot m)) - 48Cosh(h\sqrt{m}) \\
 &+ 3(1 + 4h^2m)Cosh(h\sqrt{m}))Tanh(h\sqrt{m})) \\
 B(h) &= \frac{1}{3} h \cdot \alpha \cdot Re(-Fr \cdot h^2 + \frac{(3-h^2m)r^2 Re^2 \cdot Ro^4 Sech(h\sqrt{m})^2 Tanh(h\sqrt{m})}{m^{5/2}}) \\
 C(h) &= \frac{S \cdot Re \cdot h^3 \alpha^3}{3r} \\
 D(h) &= \frac{S \cdot Re \cdot h^3 \alpha^3}{3} \\
 E(h) &= \frac{1}{24m^{5/2}} (\alpha \cdot Sech(h\sqrt{m})^4 (h\sqrt{m}(-9Fr \cdot h \cdot m^2 + 16(h^2m-3)r^2 Re^3 Ro^4 \\
 &- 4(3Fr \cdot h \cdot m^2 + 2(h \cdot m^2 - 3)r^2 Re Ro^4)Cosh(2h\sqrt{m}) - 3Fr \cdot h \cdot m^2 Cosh(4h\sqrt{m})) \\
 &+ 12(h^2m-1)r^2 Re^3 Ro^4 Sinh(2h\sqrt{m}))) \\
 F(h) &= Re \cdot S \cdot h^2 \alpha^3
 \end{aligned}$$